Pamukkale Üniversitesi Mühendislik Bilimleri Dergisi
Pamukkale University Journal of Engineering Sciences

Automated classification of wood types of acer using scanning electron microscopy images

Akçaağaç türlerinin taramalı elektron mikroskobu görüntüleri kullanılarak otomatik olarak sınıflandırılması

Eftal Sehirli[1], Hasan Sami Yaygingol[2]*

[1]Department of Computer Engineering, Engineering of Faculty, Karabük University, Karabük, Türkiye.
eftalsehirli@karabuk.edu.tr
[2]Department of Industrial Design, Safranbolu Fethi Toker Fine Arts and Design Faculty, Karabük University, Karabük, Türkiye.
hsyaygingol@karabuk.edu.tr

Received/Geliş Tarihi: 05.08.2024 Revision/Düzeltme Tarihi: 15.04.2025 doi: 10.5505/pajes.2025.87094
Accepted/Kabul Tarihi: 16.06.2025 Research Article/Araştırma Makalesi

Abstract

Wood has a key role for string instrument making. String instruments are generally made of wood types of Acer which is dominant for this issue. Accurate classification of wood types is pivotal that string instruments must be made by using high qualified materials without fraud. In this work, an innovative application was implemented to accurately classify scanning electron microscopy (SEM) images of the six different classes belonging to three different wood types of Acer. SEM images of each class were individually divided into six subregions of different sizes. 11 features were extracted on each subregion, thus creating the numerical datasets for each class. For the effectiveness of the extracted features, three feature selection techniques, namely univariate selection, feature importance and correlation matrix with heatmap were applied. SEM images of wood types of Acer were classified by machine learning (ML) models under five-fold cross validation based on two different approaches as direct classification and binary classification. The best ML model based on direct classification approach was determined as Quadratic Support Vector Machine (SVM) model with accuracy of 82.3%. General accuracy of the binary classification approach was calculated as 92.1% as a result of the collaboration of Quadratic SVM and Ensemble subspace discriminant (ESD) models. This study mainly focuses on classification of SEM images of wood types of Acer, subregion analysis, feature extraction and selection, and comparison of ML models.

Keywords: Acer, Classification, Machine Learning, SEM Images

Öz

Ahşap, yaylı çalgı yapımında kilit bir role sahiptir. Yaylı çalgılar genellikle bu konuda baskın olan Akçaağaç türlerinden yapılır. Ahşap türlerinin doğru sınıflandırılması, yaylı çalgıların sahtekarlık olmadan yüksek kaliteli malzemeler kullanılarak yapılması için çok önemlidir. Bu çalışmada, üç farklı Akçaağaç türüne ait altı farklı sınıfın taramalı elektron mikroskobu (SEM) görüntülerini doğru bir şekilde sınıflandırmak için akıllı bir uygulama geliştirilmiştir. Her bir sınıfa ait SEM görüntüleri ayrı ayrı farklı boyutlarda altı alt bölgeye ayrılmıştır. Her alt bölgede 11 özellik çıkarılmış ve her sınıf için sayısal veri kümeleri oluşturulmuştur. Çıkarılan özelliklerin etkinliği için tek değişkenli seçim, özellik önemi ve ısı haritası ile korelasyon matrisi olmak üzere üç özellik seçim tekniği uygulanmıştır. Akçaağaç türlerinin SEM görüntüleri, doğrudan sınıflandırma ve ikili sınıflandırma olmak üzere iki farklı yaklaşıma dayalı olarak beş kat çapraz doğrulama altında makine öğrenimi modelleri tarafından sınıflandırılmıştır. Doğrudan sınıflandırma yaklaşımına dayalı en iyi makine öğrenmesi modeli %82.3 doğruluk oranıyla Kuadratik DVM modeli olarak belirlenmiştir. İkili sınıflandırma yaklaşımının genel doğruluğu ise Kuadratic DVM ve Ensemble subspace discriminant (ESD) modellerinin birlikte çalışması sonucunda %92.1 olarak hesaplanmıştır. Bu çalışma temel olarak Akçaağaç türlerine ait SEM görüntülerinin sınıflandırılması, alt bölge analizi, özellik çıkarımı ve seçimi ile makine öğrenmesi modellerinin karşılaştırılmasına odaklanmaktadır.

Anahtar kelimeler: Akçaağacı, Sınıflandırma, Makine Öğrenmesi, SEM Görüntüleri

1 Introduction

Wood is the basic element of the art of string instrument making. Wood used in this art directly affects the aesthetics, condition, and tone quality of instruments. These properties of a string instrument undoubtedly play a key role in a performer's preference. From this point of view, the natural wood material used in string instrument making is an important tool which needs to be studied in different perspectives [1]. However, instrument makers claim that correct descriptive labels are not often located in string instruments and fudge can be encountered about wood materials used in string instrument making. Thus, automatic recognition applications for wood materials used in string instrument making are needed to develop.

The most important criterion to select a wood type in instrument making is its physical and chemical properties. These properties are related to macro and microstructure of wood. When they pull together, they form acoustic properties which are one of the most important aspects of tone quality of string instruments [1],[2]. Prominent trees in string instrument making are Acer and Picea trees [1]. While Acer is often used on the rib, neck, bass bar, and back side of instruments, Picea is generally utilized for making the top plate of instruments. Acer is rich in resinous channels and is therefore a good conductor of sound. These channels which seem differently in each wood and are decisive in the aesthetic appearance of the instrument determine the acoustic quality [2]. Although trees like beech, poplar, walnut, apple, and pear have been used for experimental purposes in the literature of instrument making,

*Corresponding author/Yazışılan Yazar

none of them could succeed in replacing Acer in terms of aesthetic and acoustic properties [1]. Therefore, accurate recognition applications of Acer largely used in string instruments making are particularly essential.

Even though there are a few wood types of Acer, three wood types of Acer named as Acer campestre, Acer pseudoplatanus and Acer saccharum are mainly used for string instrument making. Acer campestre is a round-topped tree that can grow up to 25 meters. It generally seems in the form of a close-branched shrub. It is heavy and dense. Acer pseudoplatanus is a smooth stem, wide and round topped tree. It can grow up to 40 meters with a diameter of maximum three meters. It is slim and well-structured as well as heavy and dense with having a polishing property. Acer saccharum is a high-density tree with a thick trunk that can grow up to 40 meters. The bird's eye is a figure found in a considerable number of Acer trees. Especially, it is likely to occur closer to the root of Acer trees [3]. Since wood types of Acer have different characteristics, it is worth the effort not only to recognize Acer but also to develop an accurate system for their automatic classification.

There have been several state-of-the-art works that apply machine learning (ML) models in order to classify images of wood types. Salma et al. [4] presented a computer program to accomplish wood identification of three wood species on microscopic images. The feature extraction was performed by daubechies wavelet method and local binary pattern (LBP). Images of wood types were classified by Support Vector Machine (SVM) with an accuracy of 85.0%. Zamri et al. [5] proposed an automated wood species recognition system for classification of 52 different wood species. Improved basic grey level auro matrix (I-BGLAM) was used for feature extraction. SVM was used to classify wood species. The accuracy of their developed system was determined as 99.8%. Filho et al. [6] suggested a two-level divide-and-conquer strategy for classification of wood species on macroscopic images. Gray-level co-occurrence matrix (GLCM), color, LBP, gabor filters, fractals, edges and local phase quantization were used for feature extraction. The accuracy of classification done by SVM was obtained as 97.8%. Yusof et al. [7] developed an application to classify 52 wood species. 157 features were extracted by using I-BGLAM and statistical properties of pores distribution (SPPD). The best accuracy was obtained as 98.69% with a kernel genetic algorithm feature selection. It is inferred that a recognition system based on ML models are conducted on wood images. Thus, scanning electron microscopy (SEM) images have the potential to investigate the wood types in a more detailed way, resulting in experimentally more reliable classification decisions.

Although there have been numerous studies regarding ML, feature extraction and classification, automated analysis and classification of the images of wood types used in string instruments making is a new challenge. Few studies have been proposed to address the fudge problem. In addition to this, the use of SEM images to handle this problem seems to be neglected. However, SEM utilized in many disciplines ensures detailed information on gray level images [8].

In this study, an intelligent application was proposed that automatically classifies the six classes belonging to three different wood types of Acer which are dominant for string instrument making. Main contributions associated with analysis and classification of SEM images of wood types of Acer can briefly be summarized as follows:

- ✓ Region analysis on SEM images of wood types of Acer was performed. This study compared subregions for wood types of Acer based on evaluation metrics and presented the optimum image size for SEM.
- ✓ 11 features frequently used in the literature were extracted on SEM images of wood types of Acer. Their effects for the classification on wood types of Acer were analyzed for the first time in this study and concluded as highly qualified.
- ✓ Three feature selection techniques were analyzed and compared in order to select the best features for the numerical dataset.
- ✓ Two different approaches based on direct classification and binary classification were minutely analyzed and compared on SEM images of wood types of Acer. This study highlights the power of binary classification on the classification of SEM images of wood types of Acer used for string instrument making. 92.1% of accuracy was obtained based on the collaboration of Quadratic SVM and ESD models.
- ✓ Effectiveness of ML models and SEM images in order to classify the six classes belonging to three different wood types of Acer were demonstrated.

2 Materials

In this study, three different wood types of Acer were divided into six classes based on quality level, texture, and regularity by an expert. A total of 300 SEM images of the same size were utilized. Each class has the same number of images, thus creating a balanced image dataset. Description of the classes is presented in Table 1.

Table 1. Description of the classes.

Class	Name	Quality Level	Texture	Regularity	City	Number of Images	Image Size
Class1	Acer campestre	low	fine-grained	symmetrical	Giresun	50	768x1024
Class2	Acer campestre	medium	fine-grained	symmetrical	Giresun	50	768x1024
Class3	Acer campestre	medium	close-grained	symmetrical	Bolu	50	768x1024
Class4	Acer pseudoplatanus	high	thick-grained	symmetrical	Sakarya	50	768x1024
Class5	Acer pseudoplatanus	high	close-grained	asymmetrical	Sakarya	50	768x1024
Class6	Acer saccharum	high	bird's eye grained	asymmetrical	Sakarya	50	768x1024

SEM was used to obtain images of each wood type of Acer and be able to bring their characteristic features into the forefront.

Each wood type was cut in the same way and had the same depth for SEM analysis. They were covered with platinum material and zoomed in 1000X during image acquisition. 50 images for each class were collected by using these procedures. An image database related to wood types of Acer was hereby created in this study. Figure 1 shows a view of each wood type of Acer before using SEM imaging. Figure 2 shows sample SEM images of each wood type of Acer.

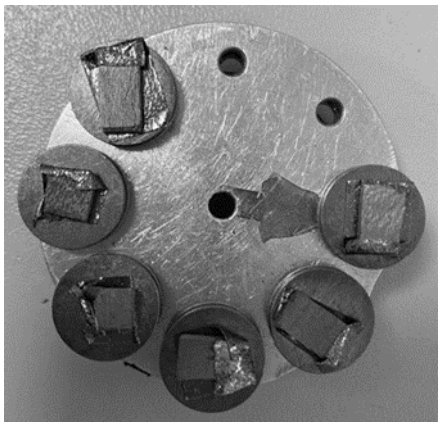

Figure 1. A view of each wood type of Acer before using SEM imaging.

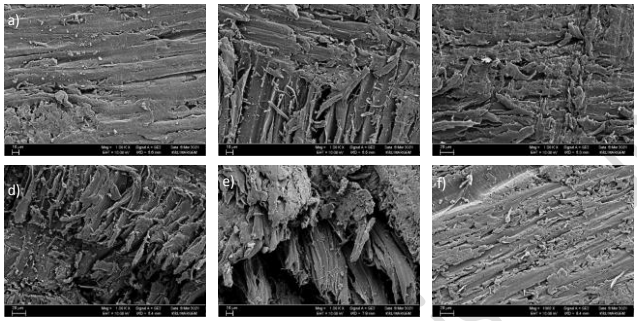

Figure 2. Sample SEM images of each wood type of Acer, a) class1, b) class2, c) class3, d) class4, e) class5, f) class6.

3 Methods

An intelligent application was developed in order to classify SEM images of wood types of Acer as Class1, Class2, Class3, Class4, Class5, and Class6. To be able to perform this task, the developed application composed of six stages, namely preprocessing, preparation of the datasets, feature extraction, feature selection, classification, and evaluation.

In the preprocessing stage, the developed application firstly accepted SEM images of wood types of Acer. The accepted images were then converted to grayscale space. Finally, because all SEM images had a rectangular annotation box at the bottom and in the same place, these boxes were automatically removed.

In the preparation of the datasets stage, six different image datasets were created by dividing images into six distinct subregions whose sizes are 100x100, 200x200, 250x250, 300x300, 500x500, and 706x1024 in pixels. Each image dataset was separated as training set and test set as 75% and 25%, respectively. After that, five-fold cross validation was performed in order to increase the stability and reliability and solve overfitting problem. This stage substantially prepared a suitable position for feature extraction process and ML models.

In the feature extraction stage, 11 features frequently used in the literature such as variance of Laplacian, entropy, gradient energy, gray level variance, gaussian derivative, thresholded absolute gradient, energy of Laplacian, spatial frequency measure, tenengrad, tenengrad variance, and sum of wavelet coefficients were calculated on each subregion of SEM images of wood types of Acer [9]-[18]. The calculation results were automatically stored into numerical datasets related to the image datasets, thus creating six different numerical datasets. As a result of this, sizes of the numerical datasets remained the same with the image datasets. Description of the created six numerical datasets is presented in Table 2.

Table 2. Description of the created numerical datasets.

Class	Size for subregion of 100x100	Size for subregion of 200x200	Size for subregion of 250x250	Size for subregion of 300x300	Size for subregion of 500x500	Size for subregion of 706x1024
Class 1	3500x11	750x11	400x11	300x11	100x11	50x11
Class 2	3500x11	750x11	400x11	300x11	100x11	50x11
Class 3	3500x11	750x11	400x11	300x11	100x11	50x11
Class 4	3500x11	750x11	400x11	300x11	100x11	50x11
Class 5	3500x11	750x11	400x11	300x11	100x11	50x11
Class 6	3500x11	750x11	400x11	300x11	100x11	50x11
Total	21000x11	4500x11	2400x11	1800x11	600x11	300x11

Variance of Laplacian serves as an autofocus measurement parameter utilized for images based on variance of image Laplacian [9]-[11]. The mathematical expression of variance of Laplacian is provided in Eq. 1.

$$\phi_{i,j} = \sum_{(i,j)\epsilon\Omega(x,y))} (\Delta I(i,j) - \overline{\Delta I})^2 \quad (1)$$

where $\overline{\Delta I}$ is the mean value of the image Laplacian, ΔI denotes the intensity value of the image Laplacian at (i,j) coordinate, Ω(x,y) refers to the coordinates of the whole image.

Entropy is an autofocus measurement parameter that indicates the state of disorder for image [9],[12]. Entropy is calculated as in Eq. 2.

$$\phi = -\sum_{i,j=1}^{\Omega(x,y)} P_{i,j}\log(P_{i,j}) \quad (2)$$

where P is the probability on (i,j)-th element, Ω(x,y) refers to the coordinates of the whole image.

Gradient energy, used as an autofocus measurement parameter, computes the sum of the squares of the image's first

derivative in both the x and y directions [9],[13],[14]. The expression of gradient energy is provided in Eq. 3.

$$\phi_{i,j} = \sum_{(i,j)\epsilon\Omega(x,y)} I_x(i,j)^2 + I_y(i,j)^2 \quad (3)$$

where I_x denotes the intensity value of the derived image based on x direction at (i,j) coordinate, I_y denotes the intensity value of derived image based on y direction at (i,j) coordinate and $\Omega(x, y)$ refers to the coordinates of the whole image.

Gray level variance is variance value of gray level image [9],[12],[13]. Gray level variance is expressed as in Eq. 4.

$$\phi_{i,j} = \sum_{(i,j)\epsilon\Omega(x,y)} (I(i,j) - \mu)^2 \quad (4)$$

where *I(i,j)* denotes the intensity value of image at (i,j) coordinate and μ is the mean value of pixels.

Gaussian derivative is an autofocus measurement parameter used in microscopy computed based on the first order Gaussian derivative along the direction of both x and y [9],[15]. The mathematical representation of Gaussian derivative is provided in Eq. 5.

$$\phi_{i,j} = \sum_{(x,y)} (I * \Gamma_x)^2 + (I * \Gamma_y)^2 \quad (5)$$

where Γ_x and Γ_y represent partial derivatives of Gaussian function. Gaussian function is expressed in Eq. 6.

$$\Gamma(x, y, \sigma) = \frac{1}{2\pi\sigma^2} \exp(-\frac{x^2 + y^2}{2\sigma^2}) \quad (6)$$

Thresholded absolute gradient composes of absolute first derivative of image in the horizontal dimension and calculates the degree of focus [9],[16]. Thresholded absolute gradient is calculated as in Eq. 7.

$$\phi_{i,j} = \sum_{(i,j)\epsilon\Omega(x,y)} [|I_x(i,j)|, \quad |I_x(i,j)|] \geq T \quad (7)$$

where *T* is used as selection of maximum value [16].

Energy of Laplacian, a focus measure parameter for both autofocus and shape from focus, refers to the second derivative of image [9],[13],[17]. The mathematical representation of energy of Laplacian is provided in Eq. 8.

$$\phi_{i,j} = \sum_{(i,j)\epsilon\Omega(x,y)} \Delta I(i,j)^2 \quad (8)$$

where ΔI refers to image Laplacian.

Spatial frequency measure is a measurement parameter for fusion of multi-local images [9],[13]. The mathematical representation of spatial frequency measure is provided in Eq. 9.

$$\phi_{i,j} = \sqrt{\sum_{(i,j)\epsilon\Omega(x,y)} I_x(i,j)^2 + \sum_{(i,j)\epsilon\Omega(x,y)} I_y(i,j)^2} \quad (9)$$

where I_x denotes the intensity value of first derivative of image based on x direction at (i,j) coordinate, I_y denotes the intensity value of first derivative of image based on y direction at (i,j) coordinate.

Tenengrad utilizes magnitude of image gradient [9],[10],[13]. Tenengrad is calculated as in Eq. 10.

$$\phi_{i,j} = \sum_{(i,j)\epsilon\Omega(x,y)} G_x(i,j)^2 + G_y(i,j)^2 \quad (10)$$

where G_x and G_y refer to the image gradient calculated based on x and y direction, respectively.

Tenengrad variance computes variance of image gradient [9],[10],[13]. The expression of tenengrad variance is provided in Eq. 11.

$$\phi_{i,j} = \sum_{(ij)\epsilon\Omega(x,y)} (G(i,j) - \bar{G})^2 \quad (11)$$

where $\bar{G}$ refers to the mean value of gradient magnitude on the whole image intensity values. G is calculated as in Eq. 12.

$$G = \sqrt{G_x^2 + G_y^2} \quad (12)$$

where G_x and G_y refer to the image gradient calculated based on x and y direction, respectively.

Sum of wavelet coefficients is an autofocus measurement parameter calculated using sub-bands in the first level discrete wavelet transform [9],[18]. The mathematical expression of sum of wavelet coefficients is provided in Eq. 13.

$$\phi = \sum_{(i,j)\epsilon\Omega_D} |W_{LH1}(i,j)| + |W_{HL1}(i,j)| + |W_{HH1}(i,j)| \quad (13)$$

where Ω_D is corresponding window of Ω in the discrete wavelet transform sub-bands, $W_{LH1}, W_{HL1}, W_{HH1}$ and W_{LL1} refer to the detail sub-bands and coarse approximation sub-bands as long as the image has been decomposed into the sub-images [9],[18].

In the feature selection stage, three different feature selection techniques were applied on the created numerical datasets in order to be able to increase accuracy, analyze the effects of the extracted features and reduce overfitting. The applied feature selection techniques are univariate selection [19],[20], feature importance [19],[21] and correlation matrix with heatmap [22].

In the classification stage, eight different ML models, namely decision tree, linear SVM, quadratic SVM, cubic SVM, k-nearest neighbor (KNN) with Euclidean distance, KNN with Minkowski distance, random forest, and ensemble subspace discriminant (ESD) were utilized to classify SEM images of wood types of Acer with the goal of the high accuracy based on direct classification and binary classification approaches. Decision tree is a supervised ML model generally used for classification problems. Decision tree generates a tree model whose leaps represents target classes [23]. SVM is a supervised ML model that can be used on linear and non-linear data to overcome classification problems. The aim of SVM is to specify the most accurate classifier line on hyper-planes for classification process by performing maximizing boundary distance [24]. KNN is a supervised ML model that calculates the nearest k points using a distance algorithm. k is a parameter which needs to be specified for this model. KNN searches for the closest class among class of nearest k-points [25]. Random forest is a supervised ML model being able to be used to achieve classification findings. Instead of using only one decision tree classifier, number of decision trees used is specified and they

are used in a random manner. Random forest calculates and identifies the decision tree with the most votes [26]. ESD is a supervised ML model used to determine a specific discriminant subspace of low dimension for classification problems [27]. Table 3 shows a brief summary about ML models and their features used in this study.

Table 3. A brief summary about ML models and their features.

ML Model	Feature
Decision Tree	Type=C4.5 learning method and Gini Diversity index
Linear SVM	Kernel function=linear, kernel scale=auto, box constraint level=1
Quadratic SVM	Kernel function=quadratic, kernel scale=auto, box constraint level=1
Cubic SVM	Kernel function=cubic, kernel scale=auto, box constraint level=1
KNN with Euclidean	Distance metric=Euclidean, k=10
KNN with Minkowski	Distance metric=Minkowski, k=10
Random Forest	Number of learners=30
ESD	Ensemble method=subspace, learner type=discriminant, number of learners=30

In the classification stage, two different approaches, researchers called as direct classification and binary classification based on ML models were employed. In the direct classification approach, a SEM image was loaded to the developed application. The loaded SEM image was directly classified based on the stages previously mentioned and only one output label was obtained out of the six classes. In the binary classification approach, a binary tree structure was designed. A SEM image was loaded to the developed application. It classified the loaded SEM image based on the stages previously mentioned and gave one output either as one of the six classes (Class A) or as class others (Class B). If the output was not class others, the classification process was to be completed. If the output was class others, the developed application would select one class and then remove it from class others. Repeatedly, the loaded SEM image was classified, and one output label was given either as one of the six classes or as class others. This process iteratively continued until the output was not class others.

In the evaluation stage, the performance metrics namely sensitivity, specificity, accuracy, and Matthews correlation coefficient (MCC) based on confusion matrix, receiver operating characteristic (ROC) curve and area under curve (AUC) were used in order to evaluate and compare the classification results obtained by ML models. Formulas of the performance metrics based on confusion matrix are presented as in Eq. 14-17. For ROC curve used as a statistical curve to compare classes, X axis of ROC curve illustrates sensitivity values while Y axis of ROC curve represents 1-specificity values. AUC is an evaluation parameter calculated based on area under ROC curve [28],[29].

$$Sensitivity = \frac{TP}{TP + FN} \tag{14}$$

$$Specificity = \frac{TN}{TN + FP} \tag{15}$$

$$Accuracy = \frac{TP + TN}{TP + TN + FP + FN} \tag{16}$$

$$MCC = \frac{(TPxTN) - (FPxFN)}{\sqrt{(TP + FP)x(TP + FN)x(TN + FP)x(TN + FN)}} \tag{17}$$

4 Experimental Results

In this study, a total of 300 SEM images in different region sizes were analyzed and classified based on two approaches, namely direct classification and binary classification. In the former, direct classification approach was implemented for the analysis on each numerical dataset, and performance metrics were calculated. Accuracy values of each ML model based on direct classification for each numerical dataset size are shown in Tables 4-9. Table 4 presents the accuracy values based on direct classification applied on the dataset size for 100x100.

Table 4. Accuracy values based on direct classification applied on dataset size for 100x100.

ML model vs Class	Class 1 Accuracy (%)	Class 2 Accuracy (%)	Class 3 Accuracy (%)	Class 4 Accuracy (%)	Class 5 Accuracy (%)	Class 6 Accuracy (%)	Overall Accuracy (%)
Decision Tree	46.5	52.0	36.5	43.6	47.3	56.0	47.0
Linear SVM	60.6	66.8	54.8	56.9	57.6	74.7	61.9
Quadratic SVM	**68.0**	**69.9**	**61.9**	**64.6**	**66.4**	**78.8**	**68.3**
Cubic SVM	55.1	65.2	53.2	45.2	42.9	64.4	54.3
KNN with Euclidean	57.2	61.1	49.0	52.9	56.6	66.8	57.3
KNN with Minkowski	57.0	60.4	48.6	53.2	57.0	66.5	57.1
Random Forest	58.9	64.8	53.2	56.2	56.7	69.2	59.8
ESD	45.0	62.5	44.3	55.2	50.1	60.8	53.0

As can be concluded from Table 4, Quadratic SVM achieved the highest overall accuracy as 68.3%. Class6 was the best distinguished class by Quadratic SVM with the accuracy of 78.8%. Table 5 presents the accuracy values based on direct classification applied on the dataset size for 200x200.

Table 5. Accuracy based on direct classification applied on the dataset size for 200x200.

ML model	Class 1	Class 2	Class 3	Class 4	Class 5	Class 6	Overall

vs Class	Accuracy (%)	Accuracy (%)	Accuracy (%)	Accuracy (%)	Accuracy (%)	Accuracy (%)	Accuracy (%)
Decision Tree	51.8	54.4	46.5	56.5	60.2	64.4	55.6
Linear SVM	66.9	71.5	68.4	70.9	66.1	80.9	70.8
Quadratic SVM	75.9	76.3	72.9	75.5	77.0	86.1	77.3
Cubic SVM	**76.1**	**76.8**	**74.6**	**75.7**	**77.0**	**86.1**	**77.7**
KNN with Euclidean	59.9	66.8	54.3	62.1	65.1	73.3	63.6
KNN with Minkowski	61.4	66.9	55.1	61.7	66.0	72.6	64.0
Random Forest	62.3	69.5	57.5	66.5	65.1	72.3	65.5
ESD	54.8	69.0	44.3	65.9	58.0	69.1	60.2

As can be concluded from Table 5, Cubic SVM achieved the highest accuracy as 77.7%. Accuracy of Class6 had higher than that of other classes. It was classified by both Quadratic and Cubic SVM with the accuracy of 86.1%. Table 6 presents the accuracy values based on direct classification applied on the dataset size for 250x250.

Table 6. Accuracy based on direct classification applied on dataset size for 250x250.

ML model vs Class	Class 1 Accuracy (%)	Class 2 Accuracy (%)	Class 3 Accuracy (%)	Class 4 Accuracy (%)	Class 5 Accuracy (%)	Class 6 Accuracy (%)	Overall Accuracy (%)
Decision Tree	57.0	59.3	50.9	58.9	65.0	70.3	60.2
Linear SVM	69.6	72.3	67.9	72.1	73.0	80.4	72.5
Quadratic SVM	75.9	75.6	75.9	78.5	77.6	85.3	78.1
Cubic SVM	**75.5**	**75.1**	**76.4**	**76.8**	**78.6**	**87.6**	**78.3**
KNN with Euclidean	63.5	66.9	55.3	64.8	65.3	75.6	65.2
KNN with Minkowski	63.4	66.5	56.0	67.3	68.5	76.6	66.4
Random Forest	64.8	70.3	58.8	65.9	69.5	75.4	67.4
ESD	60.1	69.8	45.9	68.0	65.0	73.3	63.7

As can be concluded from Table 6, Cubic SVM achieved the highest accuracy as 78.3%. Similar to Tables 4 and 5, Class6 was the best separated class by Cubic SVM with the accuracy of 87.6%. Table 7 presents the accuracy values based on direct classification applied on the dataset size for 300x300.

Table 7. Accuracy based on direct classification applied on dataset size for 300x300.

ML model vs Class	Class 1 Accuracy (%)	Class 2 Accuracy (%)	Class 3 Accuracy (%)	Class 4 Accuracy (%)	Class 5 Accuracy (%)	Class 6 Accuracy (%)	Overall Accuracy (%)
Decision Tree	55.8	66.0	50.3	67.3	66.7	74.5	63.4
Linear SVM	68.0	72.2	65.3	74.7	73.7	81.2	72.5
Quadratic SVM	**77.7**	**82.7**	**75.7**	**85.0**	**83.3**	**87.0**	**81.9**
Cubic SVM	78.3	80.7	76.7	82.5	81.7	86.8	81.1
KNN with Euclidean	62.0	68.0	55.0	67.3	69.7	79.0	66.8
KNN with Minkowski	62.3	68.2	57.3	67.2	70.8	79.8	67.6
Random Forest	67.7	72.2	60.0	72.2	72.5	80.8	70.9
ESD	62.8	72.0	47.2	69.7	68.8	76.5	66.2

As can be concluded from Table 7, Quadratic SVM achieved the highest accuracy as 81.9%. Class6 was the best distinguished class by Quadratic SVM with the accuracy of 87.0%. Table 8 presents the accuracy values based on direct classification applied on the dataset size for 500x500.

Table 8. Accuracy based on direct classification applied on dataset size for 500x500.

ML model vs Class	Class 1 Accuracy (%)	Class 2 Accuracy (%)	Class 3 Accuracy (%)	Class 4 Accuracy (%)	Class 5 Accuracy (%)	Class 6 Accuracy (%)	Overall Accuracy (%)
Decision Tree	53.0	60.5	54.0	73.5	76.5	77.5	65.8
Linear SVM	72.0	81.5	69.5	81.0	86.5	86.5	79.5
Quadratic SVM	77.0	83.0	80.0	84.0	86.5	83.5	82.3
Cubic SVM	**75.0**	**81.0**	**72.0**	**82.5**	**85.0**	**85.5**	**80.2**
KNN with Euclidean	62.0	71.0	56.0	73.5	74.0	81.5	69.7

KNN with Minkowski	65.0	70.5	53.0	73.5	77.5	80.5	70.0
Random Forest	64.0	79.0	57.0	79.0	82.5	82.5	74.0
ESD	70.5	76.0	54.0	74.5	78.0	80.0	72.2

As can be concluded from Table 8, Cubic SVM achieved the highest accuracy as 82.3%. Class5 was the best distinguished class by both Linear and Quadratic SVM with the accuracy of 86.5%. In addition to that, Linear SVM separated Class6 with the accuracy of 86.5%. Table 9 presents the accuracy values based on direct classification applied on the dataset size for 706x1024.

Table 9. Accuracy based on direct classification applied on dataset size for 706x1024.

ML model vs Class	Class 1 Accuracy (%)	Class 2 Accuracy (%)	Class 3 Accuracy (%)	Class 4 Accuracy (%)	Class 5 Accuracy (%)	Class 6 Accuracy (%)	Overall Accuracy (%)
Decision Tree	58.0	65.0	46.0	71.0	83.0	77.0	66.7
Linear SVM	65.0	77.0	63.0	82.0	83.0	82.0	75.3
Quadratic SVM	**74.0**	**82.0**	**77.0**	**85.0**	**90.0**	**84.0**	**82.0**
Cubic SVM	68.0	83.0	74.0	88.0	87.0	80.0	80.0
KNN with Euclidean	66.0	63.0	53.0	67.0	73.0	76.0	66.3
KNN with Minkowski	68.0	65.0	56.0	75.0	79.0	77.0	70.0
Random Forest	63.0	75.0	56.0	83.0	81.0	82.0	73.3
ESD	70.0	78.0	48.0	75.0	87.0	82.0	73.3

As can be concluded from Table 9, overall accuracy of Quadratic SVM was much higher than that of other ML models and obtained as 82.0%. Class5 was the best distinguished class by Quadratic SVM with the accuracy of 90.0%.

When the analysis on each image dataset was performed with direct classification, the highest classification accuracy was obtained on image dataset size for 500x500 by Quadratic SVM model. As well as accuracy, other performance metrics as sensitivity, specificity, and MCC obtained by Quadratic SVM for each class are shown in Table 10.

Table 10. Performance metrics of Quadratic SVM for each class.

	Class 1	Class 2	Class 3	Class 4	Class 5	Class 6	Overall
Sensitivity (%)	71.0	86.0	80.0	87.0	83.0	87.0	82.3
Specificity (%)	83.0	80.0	80.0	81.0	90.0	80.0	82.3
Accuracy (%)	77.0	83.0	80.0	84.0	86.5	83.5	82.3
MCC	0.54	0.66	0.60	0.68	0.73	0.67	0.65

ROC curves and AUC values of the ML models having the highest classification accuracy for each dataset are presented in Figure 3.

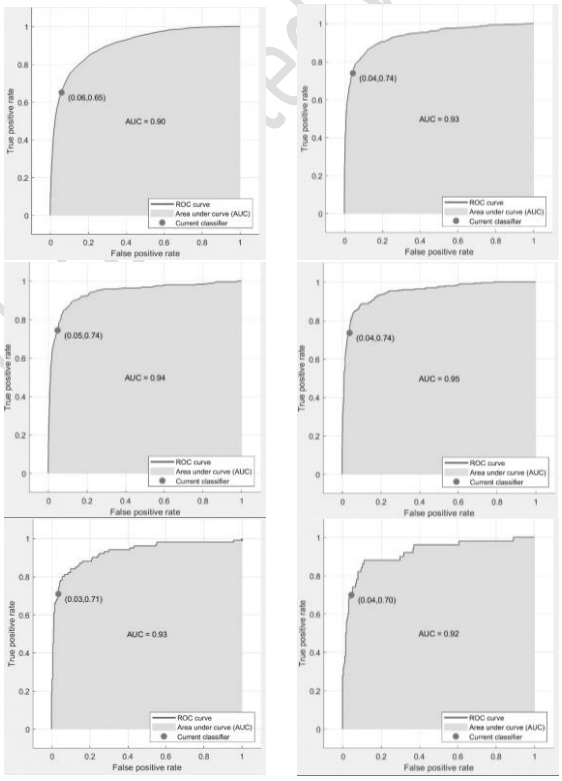

Figure 3. ROC curves and AUC values. a) Quadratic SVM for dataset size for 100x100, b) Cubic SVM for dataset size for 200x200, c) Cubic SVM for dataset size for 250x250, d) Quadratic SVM for dataset size for 300x300, e) Quadratic SVM for dataset size for 500x500, f) Quadratic SVM for dataset size for 706x1024.

When the six classes for direct classification were ranked from the best to the worst, the order was found to be Class5, Class4, Class6, Class2, Class1, and Class3, respectively. Since the highest accuracy was obtained on image dataset for 500x500, binary classification approach was performed on the same numerical datasets by organizing the classes and the number of their images in a ranked way. Description of the specified classes, accuracy, and the best ML model for binary classification are presented in Table 11.

Table 11. The description of the specified classes, accuracy, and the best ML model for binary classification.

Stage of Binary Classification	Class A	Number of Images for Class A	Class B (Class Others)	Number of Images for Class B	Accuracy (%)	The Best ML Model
1st stage	Class 5	100	Class1 Class2 Class3 Class4 Class6	100	93.5	Linear SVM
2nd stage	Class 4	100	Class1 Class2 Class3 Class6	100	94.0	Cubic SVM
3rd stage	Class 6	100	Class1 Class2 Class3	100	94.5	ESD
4th stage	Class 2	100	Class1 Class3	100	95.0	Linear SVM
5th stage	Class 1	100	Class3	100	83.5	Quadratic SVM

As can be seen from Table 11, Linear SVM distinguished Class5 from class others with an accuracy of 93.5%. Cubic SVM separated Class4 from class others with an accuracy of 94.0%. ESD marked out Class6 from class others with an accuracy of 94.5%. Linear SVM singled out Class2 from class others with an accuracy of 95.0%. Finally, Quadratic SVM separated Class1 and Class3 with an accuracy of 83.5%. The overall accuracy was obtained as 92.1%.

ROC curves and the calculated AUC values of the best ML models for each binary classification stage are shown in Figure 4. The binary tree representation of binary classification approach is presented in Figure 5.

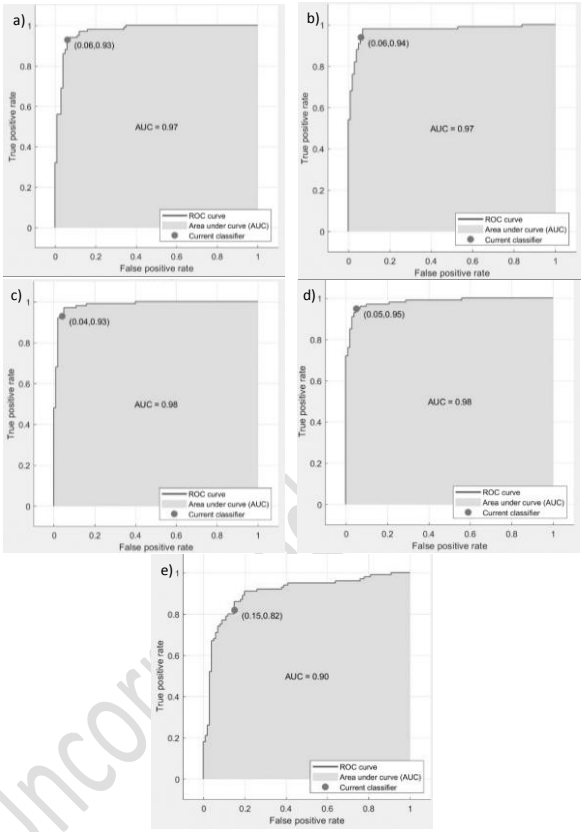

Figure 4. ROC curves and AUC values. a) Linear SVM for the 1st stage, b) Cubic SVM for the 2nd stage, c) ESD for the 3rd stage, d) Linear SVM for the 4th stage, e) Quadratic SVM for the 5th stage.

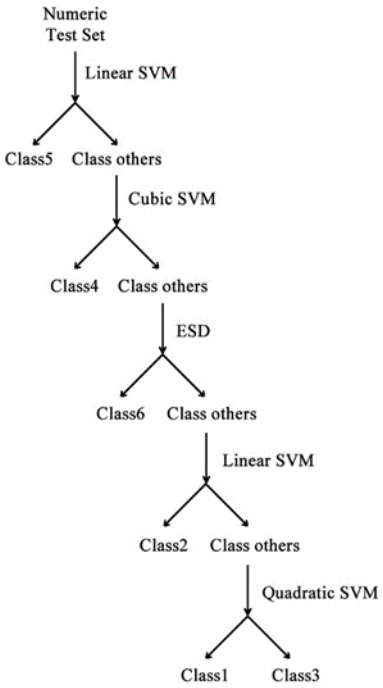

Figure 5. The binary tree representation of the binary classification approach.

11 features were automatically calculated for each subregion of the images, namely variance of Laplacian, entropy, gradient energy, gray level variance, gaussian derivative, thresholded absolute gradient, energy of Laplacian, spatial frequency measure, tenengrad, tenengrad variance and sum of wavelet coefficients. To state how the features were effective and related to each other for the classification, univariate selection, feature importance, and correlation matrix with heatmap techniques were utilized. Table 12 presents the scores of 11 extracted features calculated by univariate selection technique. Figure 6 shows the collocation of 11 features calculated by feature importance technique. Figure 7 shows the Correlation matrix with heatmap of 11 features.

Table 12. The scores of univariate selection technique.

Feature	Score
Gray level variance	1.9x1039
Tenengrad	2.0x1012
Spatial frequency measure	2.8x106
Gradient energy	4.1x105
Thresholded absolute gradient	3.7x105
Entropy	1.5x105
Sum of wavelet coefficients	3.8x103
Energy of Laplacian	6.5x102
Tenengrad variance	6.5x102
Gaussian derivative	6.0x102

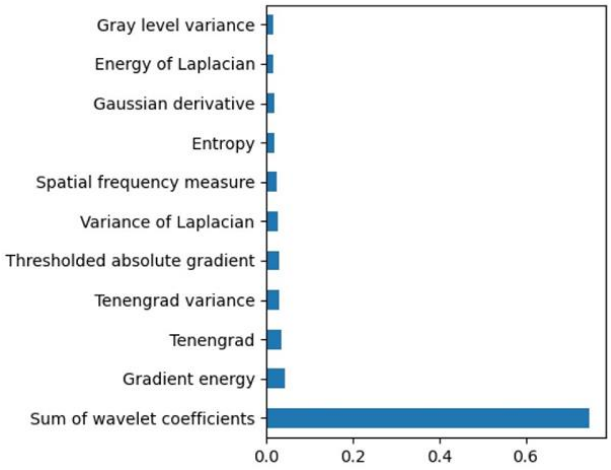

Figure 6. The scores of feature importance technique.

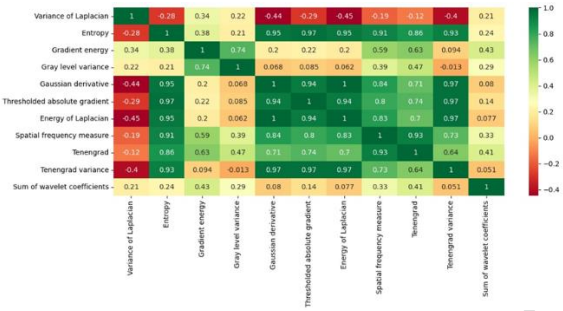

Figure 7. Correlation matrix with heatmap of 11 features.

5 Discussion

In this study, an intelligent application was developed for people working in the music industry in order to obtain information about quality and suitability of wood types of Acer before making and buying string instruments. 300 SEM images of wood types of Acer were analyzed performing stages as preprocessing, preparation of the datasets, feature extraction, feature selection, classification, and evaluation. The experimental results demonstrated that 11 extracted features were necessary to collect information on SEM images of wood types of Acer for the classification. It was presented that two different approaches called direct classification and binary classification were compatible in classifying SEM images of wood types of Acer. The overall accuracy was obtained as 82.3% on dataset size 500x500 in pixels for direct classification. The overall accuracy reached 92.1% on dataset size 500x500 in pixels for binary classification. The obtained results pointed out that binary classification outperformed direct classification in terms of performance metrics.

In this study, region analysis on SEM images of wood types of Acer was performed. The SEM images were divided into six different subregions such as 100x100, 200x200, 250x250, 300x300, 500x500, and 706x1024 in pixels. The subregion 500x500 in size was more prominent and effective to extract information and recognize wood types of Acer for both direct classification and binary classification. It was obtained that smaller size subregions were not sufficient to classify and extract information related to wood types of Acer. The accuracy difference between datasets whose subregions are 500x500 and 706x1024 was in minor level as 0.03%. Quadratic SVM model was the most successful classifier for both.

11 features were extracted from SEM images and used to classify wood types of Acer. Table 12, Figure 5, and Figure 6 showed that they were related to each other in order to classify images with a high accuracy. According to univariate selection technique, gray level variance was the most significant feature and Gaussian derivative was the least important feature. All features, however, had a positive effect on the dataset. When one or a few of them were removed from the dataset and classification was performed by ML models, the obtained results showed that overall accuracy and MCC scores decreased dramatically.

For the feature importance technique, sum of wavelet coefficients was the most valuable feature and gray level variance was the least valuable feature. Nevertheless, similar to univariate selection technique, all features were favorable on the dataset. When some of them were eliminated from the dataset and ML models performed the classification, it was uncovered that performance metrics decreased prominently.

While entropy was the most prominent feature, variance of Laplacian was the least effective feature based on correlation matrix with heatmap. When variance of Laplacian was removed from the dataset and classification was performed with ten measurement features, it was observed that overall accuracy decreased under 90.0%. Thus, variance of Laplacian was included for the dataset. As a result of them, all of 11 features were selected and used for the dataset.

The developed application was compared with the state-of-the-art works. Table 13 presents the comparison based on number of classes, size of the used dataset, the ML classifier and the obtained accuracy.

Table 13. Comparison between state-of-the-art works and the developed application [30].

Author	Year	Number of classes	Dataset Size	Classifier	Accuracy (%)
Salma et al. [4]	2018	3	4320	SVM	85.0
Zamri et al. [5]	2016	52	5200	SVM	99.8
Filho et al. [6]	2014	41	2942	SVM	97.8
Martins et al. [31]	2013	112	2240	LDA	80.7
Yadav et al. [32]	2013	25	500	MLP	92.6
Yusof et al. [7]	2013	52	5200	LDA	98.7
Filho et al. [33]	2010	22	1270	MLP	80.8
Yusof et al. [34]	2010	30	3000	MLP	90.3
Nasirzadeh et al. [35]	2010	37	3700	NN	96.6
Yusof et al. [36]	2009	20	2010	NN	91.0
Tou et al. [37]	2009	6	12	KNN	85.0
Tou et al. [38]	2008	5	500	MLP	72.8
Khalid et al. [39]	2008	20	2100	MLP	95.0
Tou et al. [40]	2007	5	250	MLP	72.0
The developed application	2022	6	600	Quadratic SVM and ESD	92.1

According to Table 13, the developed application outperforms the other state-of-the-art works when the number of classes is six or lower. As the dataset size expands, it is observed that it has a positive effect on accuracy. When the dataset is lower than 600, the developed application is almost the best based on accuracy. This study ensures that ML models and the frequently used 11 features are suitable for the classification of SEM images of wood types of Acer. This paper presents that the developed application has a novel method applying binary classification approach based on the collaboration of Quadratic SVM and ESD models for the classification of SEM images of wood types of Acer.

The developed application provides people with getting information related to string instruments. As can be claimed by instrument makers about misstatement and distortion cases related to string instruments, people may buy and use many fake string instruments. To prevent or minimize these cases, the developed application can be used to validate wood types of Acer which is a prominent wood for string instruments making. However, there are two limitations for the developed application. The first one is to be able to analyze six classes-based Acer-made instruments. The second one is to accept SEM images of wood types of Acer. Obtaining SEM images in order to analyze an Acer-made instrument is a little challenging and costly.

As a future work, another imaging system will be used to collect images of wood type of Acer in a faster way. A mobile application will be developed to get information about wood type of Acer used for any string instruments. Therefore, before buying a new string instrument, a person can validate the used wood type of Acer. In addition to that, although Acer is the most effective tool for string instruments [1], images of other wood types used for string instruments will be analyzed and compared with wood types of Acer. Deep learning models and different numerical datasets including various extracted features for ML models will be able to be used to conduct the analysis and classification of wood types used for string instruments.

6 Conclusion

This study presents a developed application in order to analyze wood types of Acer prominently used for string instrument making. The most frequently used six wood types of Acer were selected and investigated. SEM images of these wood types of Acer were classified by using ML models based on binary and direct classification approaches. For this task, 11 features were extracted to create the numerical dataset and their effectiveness were validated after performing three feature selection methods. In addition to them, region analysis on SEM images were analyzed. It was pointed out that accuracy of the binary classification approach reached to highest score as 92.1% as a result of the collaboration of Quadratic SVM and ESD models on 500x500 subregion. This application can be a helper tool for people in string instrument industry.

7 Ethics Committee Permission and Conflict of Interest

Ethics committee permission is not required for the prepared article.

There is no conflict of interest with any person/institution in the prepared article.

8 Credit Author Statement

Author 1:

Conceptualization, Data curation, Formal analysis, Literature survey, Methodology, Project administration, Software, Validation, Writing – original draft, Writing – Review & Editing.

Author 2:

Conceptualization, Data acquisition, Formal analysis and investigation, Literature survey, Resources, Visualization, Writing – original draft, Writing – Review & Editing.

9 References

[1] Yaygingol HS. *Yaylı Çalgı Yapım Teknolojisi*, Üçüncü baskı, Eskişehir, Türkiye, Anadolu Üniversitesi Yayınları, 2010.

[2] Nicolini G, Scolari G. *Come Nasce un Violin*, Cremona, Italy, Edizioni Stradivari, 1985.

[3] Gökmen H. *Kapalı tohumlular – Angiospermae*, Ankara, Türkiye, Orman Harita ve Fotogrametri Müdürlüğü, 1977.

[4] Salma Gunawan PH, Prakasa E, Sugiarto B, Wardoyo R., Rianto Y, Damayanti R, Krisdianto Dewi LM. "Wood identification on microscopic image with daubechies wavelet method and local binary pattern". *International Conference on Computer, Control, Informatics and its Applications*, Tangerang, Indonesia, 1-2 November 2018.

[5] Zamri MIP, Khairuddin ASM, Mokhtar N, Yusof R. "Wood species recognition system based on improved basic grey level aura matrix as feature extractor". *Journal of Robotics, Networking and Artificial Life*, 3(3), 140-143, 2016.

[6] Filho PLP, Oliveira LS, Nisgoski S, Britto Jr. AS. "Forest species recognition using macroscopic images". *Machine Vision and Applications*, 25, 1019–1031, 2014.

[7] Yusof R, Khalid M, Khairuddin ASM. "Application of kernel-genetic algorithm as nonlinear feature selection in tropical wood species recognition system". *Computers and Electronics in Agriculture*, 93 68–77, 2013.

[8] Mohamed A, Abdullah A. "Scanning electron microscopy (SEM): a review". *2018 International Conference on Hydraulics and Pneumatics – HERVEX*, Baile Govora, Romania, 7-9 November 2018.

[9] Pertuz S, Puig D, Garcia MA. "Analysis of focus measure operators in shape-from-focus". *Pattern Recognition*, 46(5), 1415–1432, 2012.

[10] Pech-Pacheco J, Cristobal G, Chamorro-Martinez J, Fernandez-Valdivia J. "Diatom autofocusing in bright field microscopy: a comparative study". *15th International Conference on Pattern Recognition*, Barcelona, Spain, 3-7 September 2000.

[11] Kavsaoğlu AR, Sehirli E. "A novel study to classify breath inhalation and breath exhalation using audio signals from heart and trachea". *Biomedical Signal Processing and Control*, 80, 1-9, 2023.

[12] Firestone L, Cook K, Culp K, Talsania N, Preston Jr. K. "Comparison of autofocus methods for automated microscopy". *Cytometry*, 12, 195–206, 1991.

[13] Huang W, Jing Z. "Evaluation of focus measures in multi-focus image fusion". *Pattern Recognition Letters*, 28(4), 493–500, 2007.

[14] Malik AS, Choi TS. "A novel algorithm for estimation of depth map using image focus for 3D shape recovery in the presence of noise". *Pattern Recognition*, 41(7), 2200–2225, 2008.

[15] Geusebroek J, Cornelissen F, Smeilders A, Geerts H. "Robust auto focusing in microscopy". *Cytometry*, 39, 1–9, 2000.

[16] Santos A, de Solorzano CO, Vaquero JJ, Pena JM, Mapica N, Pozo FD. "Evaluation of auto focus functions in molecular cytogenetic analysis". *Journal of Microscopy*, 188(3), 264–272, 1997.

[17] Sun Y, Duthaler S, Nelson BJ. "Auto focusing in computer microscopy: selecting the optimal focus algorithm". *Microscopy Research and Technique*, 65(3), 139–149, 2004.

[18] Yang G, Nelson B. "Wavelet-based autofocusing and unsupervised segmentation of microscopic images". *IEEE/RSJ International Conference on Intelligent Robots and Systems*, Las Vegas, USA, 27-31 October 2003.

[19] Guyon I, Elisseef A. "An introduction to variable and feature selection". *Journal of Machine Learning Research*, 3, 1157–1182, 2003.

[20] Jain S, Saha A. "Rank based univariate feature selection methods on machine learning classifiers for code smell detection". *Evolutionary Intelligence*, 15, 609-638, 2022.

[21] Opoku Asare K, Terhorst Y, Vega J, Peltonen E, Lagerspetz E, Ferreira D. "Predicting depression from smartphone behavioral markers using machine learning methods, hyperparameter optimization, and feature importance analysis: exploratory study". *JIMR Mhealth Uhealth*, 9(7), 1-17, 2021.

[22] Zhend A, Casari A. *Feature engineering for machine learning: principles and techniques for data scientists*, 1st ed. O'Reilly, USA, 2018.

[23] Turan MK, Sehirli E. "A novel method to identify and grade DNA damage on comet images". *Computer Methods and Programs in Biomedicine*, 147, 19–27, 2017.

[24] Ozdemir R, Turanli M. "Comparison of machine learning classification algorithms for purchasing forecast". *Journal of Life Economics*, 8, 59–68, 2021.

[25] Güvenç E, Çetin GC, Koçak H. "Comparison of KNN and DNN classifiers performance in predicting mobile phone price ranges". *Advances in Artificial Intelligence Research*, 1, 19–28, 2021.

[26] Akar Ö, Güngör O. "Rastgele orman algoritması kullanılarak çok bantlı görüntülerin sınıflandırılması". *Journal of Geodesy and Geoinformation*, 1(2), 139–146, 2012.

[27] Ashour AS, Guo Y, Hawas AR. "Ensemble of subspace discriminant classifiers for schistosomal liver fibrosis staging in mice microscopic images". *Health Information Science and Systems*, 6(1), 1-10, 2018.

[28] Fawcett T. "An introduction to ROC analysis". *Pattern Recognition Letters*, 27(8), 861–874, 2006.

[29] Powers DMW. "Evaluation: from precision, recall and f-measure to ROC, informedness, markedness & correlation". *International Journal of Machine Learning Technologies*, 2(1), 37–63, 2011.

[30] Kryl M, Danys L, Jaros R, Martinek R, Kodytek P, Bilik P. "Wood recognition and quality imaging inspection systems". *Journal of Sensors*, 2020, 1-19, 2020.

[31] Martins J, Oliveira LS, Nisgoski S, Sabourin R. "A database for automatic classification of forest species". *Machine Vision and Applications*, 24, 567–578, 2013.

[32] Yadav AR, Dewal ML, Anand RS, Gupta S. "Classification of hardwood species using ANN classifier". *Fourth National Conference on Computer Vision, Pattern Recognition, Image Processing and Graphics*, Jodhpur, India, 18-21 December 2013.

[33] Filho PLP, Oliveira LS, Britto AS. "Forest species recognition using color-based features". *20th International Conference on Pattern Recognition*, Istanbul, Turkey, 23-26 August 2010.

[34] Yusof R, Rosli NR, Khalid M. "Using Gabor filters as image multiplier for tropical wood species recognition system". *12th International Conference on Computer Modelling and Simulation*, Cambridge, UK, 24-26 March 2010.

[35] Nasirzadeh M, Khazael AA, Khalid MB. "Woods recognition system based on local binary pattern". *2nd International Conference on Computational Intelligence, Communication Systems and Networks*, Liverpool, UK, 28-30 July 2010.

[36] Yusof R, Rosli NR, Khalid M. "Tropical wood species recognition based on Gabor filter". *2nd International Congress on Image and Signal Processing*, Tianjian, China, 17-19 October 2009.
[37] Tou JY, Tay YH, Lau PY. "A comparative study for texture classification techniques on wood species recognition problem". *Fifth International Conference on Natural Computation*, Tianjian, China, 14-16 August 2009.
[38] Tou JY, Tay YH, Lau PY. "One-dimensional grey-level co-occurrence matrices for texture classification", *International Symposium on Information Technology*, Kuala Lumpur, Malaysia, 26-28 August 2008.
[39] Khalid M, Lee ELY, Yusof R, Nadaraj M. "Design of an intelligent wood species recognition system". *International Journal of Simulation: Systems, Science and Technology*, 9(3), 9–19, 2008.
[40] Tou JY, Lau PY, Tay YH. "Computer vision-based wood recognition system". *International Workshop on Advanced Image Technology*, 2007.